Integration of remote sensing data for forest risk assessment and disturbance monitoring in the Krkonoše National Park

Authors:
Vojtěch Bárta[1], Lucie Homolová[1], Petr Lukeš[1], Lucie Červená[2], Jakub Lysák[2], Zuzana Lhotáková[3], Eva Neuwirthová[3], Jana Albrechtová[3], Markéta Potůčková[2], Lucie Kupková[2]

[1] Global Change Research Institute of the Czech Academy of Sciences, Department of Remote Sensing, Bělidla 986/4a, 603 00 Brno

[2] Department of Applied Geoinformatics and Cartography, Faculty of Science, Charles University, Albertov 6, Prague, Czech Republic

[3] Department of Plant Experimental Biology, Faculty of Science, Charles University, Viničná 5, Prague, 12800, Czech Republic

Corresponding author:
Vojtěch Bárta barta.v@czechglobe.cz

Abstract

Forest disturbances are a natural phenomenon, however, understanding of their spatial progression is essential to adapt appropriate management strategies. Because most disturbances are to some extent influenced by management measures, it is necessary to study disturbances in areas with minimal human interference. This study aims to detect and analyse the progress of disturbance in and around a non-intervention zone of the Krkonoše National Park in the Czech Republic. Our analysis showed that either Sentinel-2 based or airborne-based approach was able to detect ongoing disturbances, however, spatial resolution is a key parameter for the detection of small-scale forest disturbances. Both sources independently identified a distance of up to 125 m from previous disturbances as the area with the highest risk of further propagation. The specific distance depends on the phase of disturbance at the site. The distance is lower in areas experiencing a progressive disturbance phase (i.e. 75 m in areas with a high population density of bark beetles). A sequence of remote sensing detection and buffer zone creation could be used as a tool for assessing risk areas in forest stands.

Keywords

Forest disturbances; nature protection zones; bark beetle; airborne hyperspectral images; Norway spruce

1. Introduction

Forest disturbances, natural (due to droughts, windthrows, fires, insect outbreaks etc.) and anthropogenic (management activities, logging), are integral part of forest ecosystem dynamic. The regime of natural disturbance has recently changed as their occurrence and severity has increased due to climate change impacts (Patacca et al., 2023; Seidl et al., 2017, 2011). Disturbances by drought and wind are often trigger points for other disturbances caused by fires and insects (Seidl et al., 2017). The most important disturbance agent in European forests is wind, followed by fire and bark beetle (*Ips typographus, L.*) (Thom et al., 2013). The bark beetle disturbance doubled its share of the total damage in the last 20 years (Patacca et al., 2023). The bark beetle is a significant forest insect pest, primarily attacking mature Norway spruce (*Picea abies* (L.) H. Karst) and plays a not negligible role in shaping forest dynamics (Wermelinger, 2004). Outbreaks of *Ips typographus* typically begin with the colonization of weakened or wind-thrown Norway spruce trees. This pattern is typical of a low and stable population level, known as the endemic phase (Hlásny et al., 2019; Wermelinger, 2004). During this stage, most beetles disperse by moving a few hundred metres per generation. However, rare individuals can travel over a kilometre. The particular distance depends on the availability of susceptible breeding material and population density. The distance between newly attacked trees is shorter during the epidemic phase (Hlásny et al., 2019; Økland et al., 2016; Wermelinger, 2004). Due to the spatial nature of bark beetle spread, much of the research has focused on identifying areas at a higher risk of infestation. Doležal et al. (2016) tested this distance using pheromone traps to catch marked beetles. Byers et al. (2000) tested bark beetle dispersal using a model to simulate their flying capabilities. Other studies employed aerial or satellite imagery (Kautz et al., 2011; Lausch et al., 2012; Potterf et al., 2019), airborne laser scanning (Stereńczak et al., 2014), or ground-based true data observation (Stadelmann et al., 2014). As Norway spruce is a cornerstone species of the timber industry in many countries, bark beetle outbreaks may have severe economic impacts on the forestry sector (Hlásny et al., 2021b; Montagné-Huck & Brunette, 2018). Although bark beetle outbreaks may contribute positively to biodiversity by creating diverse habitat structures (Müller et al., 2008; Vrba et al., 2024), their overall impact negatively influences ecosystem services and reduces forest carbon storage capacity (reviewed by Hlásny et al., 2021a).

In the Czech Republic, about 34.2% of the country is covered by forests, with about 46% of that being Norway spruce dominated, productive forests (MZE, 2024). The transformation of Europe's natural mixed broadleaved forests into monoculture conifer plantations, particularly with Norway spruce and Scots pine (*Pinus sylvestris* L.), has been well-documented over the past few centuries (Kirby & Watkins, 2015). Norway spruce stands were often planted outside its optimum environmental conditions, i.e. in the lower elevations. With rapidly changing climate in recent decades, spruce trees have become less resilient to more frequent and extreme weather conditions such as windstorms, drought episodes (Brázdil et al., 2022) and have been losing their productive potential (Kusbach et al., 2025). The last massive bark beetle outbreak, starting around 2015, is considered as the most disastrous disturbance to Norway spruce forests over the territory of the Czech Republic in documented history (Brázdil et al., 2022; T. Hlásny et al., 2021b; Zahradník & Zahradníková, 2019). A Similar finding was reported from Germany, Austria or Slovakia (Hallas et al., 2024; Senf & Seidl, 2021).

The dynamics of bark beetle outbreaks are different in nature protected areas, such as national parks, where forest management is limited or entirely absent, than in intensively managed forests, where salvage operations are used to suppress infestations. Moreover, areas with restricted management can become a trigger for a larger outbreak, especially after severe windstorms, when many dead trees are left uncleared. This has been documented in the past, for example in the Tatra National Park in Slovakia after the storm in 2004 (Nikolov et al., 2014; Potterf et al., 2019). Due to difficult terrain with a large elevation gradient, limited number of human resources and limited management interferences in the nature protection zones, the remote sensing-based methods have become a useful tool for monitoring disturbances in those areas (Bijou et al., 2023; Drechsel & Forkel, 2025; Senf et al., 2017). In combination with traditional forest monitoring methods, such as field surveys, more accurate and timely detection of disturbances can be achieved (Bárta et al., 2021). Studying the spatial distribution could help identify areas at high risk of disturbance spread in the following years, allowing forest management measures to be targeted at these areas (Kautz et al., 2011).

Our study is therefore focused on remote sensing monitoring of forest disturbances (most likely bark beetle induced) and identification of potential hotspots for further spreading in the Krkonoše National Park in the Czech Republic. Specific research questions are formulated as follows: 1) What potential do satellite- and airborne-based systems offer for forest disturbance detection? 2) Which surrounding areas are at risk of further disturbance spread, and at what distance is the search for new disturbances most effective?

2. Material and methods

2.1. Study area

Study area is located in the Krkonoše National Park (KRNAP), the mountain range situated at the border between the Czech Republic and Poland (Fig. 1). KRNAP is the oldest national park in the Czech Republic and protects the relics of the tundra ecosystems and unique mosaic of natural alpine meadows, wetlands and forests in Central Europe. The area has a cold and humid climate, with mean annual temperatures 3.7 °C, and mean annual precipitation of 1 346 mm (average values for the period 1991 – 2020 extracted for Pec pod Sněžkou area from the ClimRisk portal; ClimRisk, 2025). Forests cover approximately 85% of the park area and are dominated by Norway spruce stands, with remnants of natural beech-fir and mixed montane forests at lower altitudes. The area of interest covers the highest parts of the national park around the municipality of Pec pod Sněžkou, including the catchments of Horní Úpa and Horní Čistá streams (Fig. 1). The area of interest is approximately 90 km^2 (about one quarter of the national park) that was fully covered by airborne hyperspectral images and lidar data in 2022. The data acquisition was repeated in two sub-areas with different progress of disturbance in 2024. Sub-area A is situated at higher elevation (800–1300 m a.s.l.) and is dominated by natural and near-natural spruce stands. Due to the non-intervention management regime, the area is at increased risk of bark beetle outbreaks, which caused significant damages in recent years. Therefore, in our study this sub-arearepresents a forest in a later stage, progressing disturbance. While sub-area B, which is situated at an elevation of 800–1000 m a.s.l.,falls within the concentrated management zone, with a smaller portion of near-natural spruce stands. The area has been regularly affected by bark beetle outbreaks, although their intensity has been mitigated by active management interventions. In our study represents an incipient stage of disturbance.

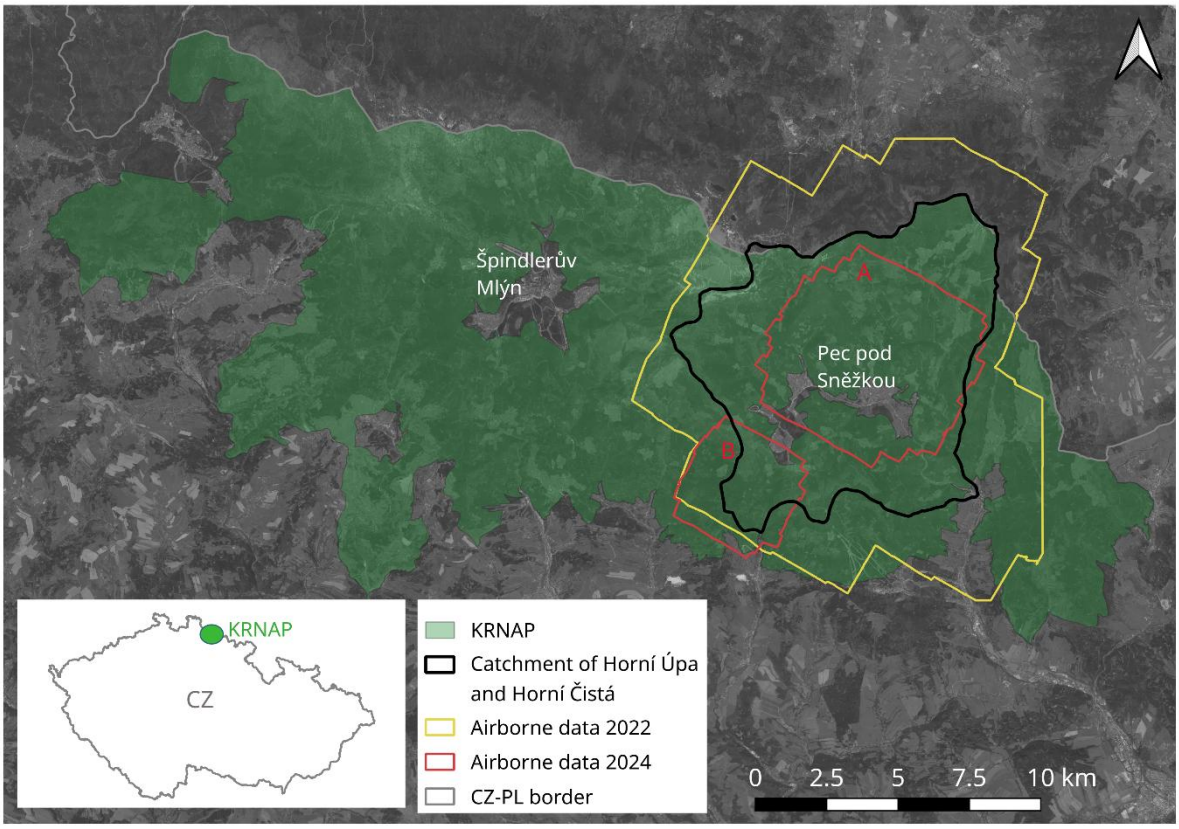

Fig. 1. *Overview of the study area and the coverage of the airborne data in 2022 and 2024. Airborne data in 2024 with higher spatial resolution were collected for two sub-areas, the central part labelled as A, and the southern part labeled as B.*

2.1. Remote sensing data and processing

2.2.1. Airborne data

Airborne hyperspectral and laser scanning data were acquired with the Flying Laboratory of Imaging Systems (Hanuš et al., 2023) operated by the Global Change Research Institute. The flying laboratory has on board a laser scanner LMS Q780 from Riegl and two imaging spectroradiometers from Itres Ltd., the CASI sensor covers the visible and near infrared range (VNIR 400 - 1000 nm), the SASI sensor covers the shortwave infrared range (SWIR 1000 - 2500 nm). Two airborne campaigns took place on sunny, cloud-free days on 19 July 2022 and 30 July 2024. Airborne images from July 2022 cover the entire area of interest in a single mosaic with the spatial resolution of 2 m per pixel in VNIR and 5 m per pixel in SWIR. The second airborne image acquisition from July 2024 covers about 70% of 2022 flights, because we

focused on two sub-areas with different progress of disturbance. There we preferred higher spatial resolution (0.5 m per pixel in VNIR and 1.25 m per pixel in SWIR).

Airborne hyperspectral data were pre-processed, including radiometric, georeferencing and atmospheric correction using the methods described in Hanuš et al. (2023). Vicarious calibration using a ground-measured reference target was used to improve the atmospheric correction. Spectral bands affected by water vapour absorption or by low signal-to-noise ratio (i.e. at the beginning (<450 nm) and the end (>2300 nm) of the spectral range) were discarded from further analysis.

Airborne laser scanning data were processed into digital surface model (DSM) and canopy height model (CHM) following the processing chain described in Hanuš et al. (2023). The spatial resolution of lidar-based products was equal to the spatial resolution of the VNIR images.

2.2.2. Satellite data

Sentinel-2 imagery, processed to Level-2A surface reflectance, was used to construct annual cloud-free mosaic over the study area from 2017 up to 2024. Sentinel-2 imagery was chosen due to its high spatial resolution (20 m pixel size), frequent revisit time (5 days), and freely accessible data, making it highly suitable for annual assessments of forest disturbances. These yearly mosaics were generated from Sentinel-2 observations acquired during the summer months, specifically from June 1st to August 30th. The summer period was selected due to higher illumination angles, minimal shadow effects, and peak vegetation phenological stages, thus enhancing comparability between annual composites. For each year, a median composite of surface reflectance values was computed from all-available images after applying per-pixel cloud mask using the Sentinel Hub Cloud Detector (Sentinel Hub, 2025). The result is a time series consisting of seven cloud-free mosaics, each representing the summer median surface reflectance across the KRNAP study area. The entire workflow for generating cloud-free composites was fully automated using Google Earth Engine (GEE) cloud computing environment (Gorelick et al., 2017).

These annual cloud-free mosaics were subsequently used to compute the Disturbance Index (DI) according to Healey et al. (2005). The Disturbance Index was selected over alternative indices like NDVI or NBR because its multidimensional integration of Tasseled Cap components (Brightness, Greenness, and Wetness) provides enhanced sensitivity to the complex spectral signatures of bark beetle-induced mortality, capturing both vegetation loss

and exposure of non-photosynthetic materials. The DI has been specifically validated for bark beetle detection in Central European spruce forests, with Kupková et al. (2018) demonstrating its effectiveness in similar mountainous conditions.

Each component, Brightness (B), Greenness (G) and Wetness (W), was then normalized by subtracting mean (μ) and dividing by the standard deviation (σ), where these statistics were calculated exclusively from forested pixels within the study area (eq. [1]). Forest mask was calculated from a high-resolution forest border layer produced by the Czech Forestry Institute. Normalization of the Tasseled Cap components ensured that DI values were comparable across years and scenes by minimizing the influence of varying atmospheric conditions, illumination, and sensor differences. This step standardizes the data to a common scale, enhancing the temporal consistency and spatial transferability of disturbance detection results Healey at al. (2005). Normalization was based exclusively on forest pixels to ensure that the calculated mean and standard deviation reflect only the spectral characteristics of undisturbed forest, which is the reference baseline for detecting disturbances.

$$X_r = (X - X_{\mu})/X_{\sigma} \quad [1]$$

Here, X corresponds to one of the three Tasseled Cap components (B, G, or W). The DI was subsequently derived from these normalized components as follows:

$$DI = B_r - G_r W_r \quad [2]$$

The resulting annual DI series enabled identification of forest degradation and disturbances. To enhance the robustness and reliability of disturbance detection, short-term DI trends were analysed by computing trend slopes using non-parametric Theil-Sen regression (Sen's slope) over three periods: 2017-2022, 2017-2023, and 2017-2024. The Theil-Sen regression was employed for short-term trend analysis due to its robustness against outliers and insensitivity to non-normal data distributions, characteristics common in satellite-derived indices such as DI. This analysis was also automated within the GEE environment. For further analyses, we worked with the slope component of the regression line (refers to as DI slope value). These DI-based short-term trends provide an effective early-warning mechanism for forest managers, facilitating rapid identification of degraded or disturbed areas and enabling targeted management interventions.

To precisely locate disturbances within actual forest areas, the satellite-derived DI trend data at 20 m resolution were resampled to the spatial resolution of the VNIR data and then compared to lidar-based CHM with high spatial resolutions of 2 m (2022 dataset) and 0.5 m (2024 dataset).

Using these high-resolution CHMs, a fine-scale forest mask was created to exclude non-forest areas (e.g. smaller meadows, timber stacks, construction zones, and old clearcuts) from further analysis. The forest mask excluded pixels corresponding to canopy heights below 4 m, thereby removing disturbances in very young forests, and above 50 m, which helped eliminate artificial structures and errors inherent in the canopy height model data.

2.3. Detection of disturbances from airborne data

The detection of forest disturbance from the airborne data focused on identification of dead standing trees. It was based on a two-class classification (healthy and dead standing trees) that was performed by a decision tree algorithm. This method was more accurate than other supervised classification methods such as Support Vector Machine, K-Nearest Neighbour or Discriminant analysis, which were also tested on the training dataset (i.e., the classification accuracy was lower by 6%, 3% and 1%, respectively, compared to the decision tree). The classification algorithm was employed on both VNIR and SWIR data, being more accurate on the VNIR data with higher spatial resolution than the merged VNIR and SWIR data. Therefore, we further proceed with the classification on VNIR data only. Due to the change in spatial and spectral resolution of hyperspectral data in 2022 and 2024, the models were trained on manually selected trees' canopies for each hyperspectral data separately. An overall accuracy of 87% was achieved in the classification of healthy and dead trees for the 2022 airborne data, and 95% for the 2024 data.

To minimize false detections the same forest mask using the height thresholds (<4 m & >50 m) as for the satellite data were used. The results of disturbance detection from the airborne hyperspectral data were used as reference data for verification of disturbances from satellite data.

2.4. Concept of buffer zones and assessment of spatial patterns

The correspondence of disturbance identification in both data sources (satellite and airborne) can serve as a measure of robustness and reliability of the detection. Because these two detections cannot be exactly spatially aligned due to geolocation error in mountainous areas. European Space Agency (ESA) reports that in most cases the geolocation error of Sentinel-2 images is between 7–12 m (Copernicus Service, 2021), but in some cases we found a spatial misalignment of 40 m between satellite and airborne detected disturbance on very steep slopes. The differences in the spatial resolution or coordination systems of remote sensing data require additional transformations before the data can be processed automatically. Each transformation

introduces errors into the data, thus increasing its inaccuracy. Therefore, the buffer zones were built around each detection source from satellite or aerial hyperspectral data at distances from the epicentre. The buffer zones were constructed as a ring-shaped curves around detected disturbances at specific distances from 25 to 200 m with the step of 25 m, e.g. buffer zone r = 50 m refers to the area starting at the boundary of the previous zone (i.e. buffer zone r = 25 m) and extending up to a distance of 50 m from the centre of the disturbance. The forest workers in productive forests in Central Europe use the similar strategy to find newly colonized trees by bark beetles (Hlásny et al., 2019), most of them are located a few tens of meters from previous bark beetle hotspots.

3. Results

3.1. Detection of disturbances

The detection of dead standing trees from the airborne data revealed the total area under disturbances reaching 10.05 ha in the sub-area A in 2022, subsequently it almost doubled the extent up to 18.84 ha in 2024. Most detections were located on south-oriented slopes within the sub-area A in the locality of 'Koule' (Fig. 2), where the greatest progression was recorded as well. The first disturbances on this site were already spotted by forest workers before the first airborne data acquisition (i.e. before 2022) and were related mostly to infestation by spruce bark beetles. In contrast to this, the sub-area B contained only a few isolated disturbance spots, formed by individual trees or small tree clusters, representing a total area of 0.78 ha in 2022 and 1.5 ha in 2024. Any larger disturbance in terms of size was not detected by field workers before 2022.

In both cases at sub-area A and B, the total area affected by disturbance is underestimated because the detection considered only sun-lit parts of forest. It is shown in Fig. 2, where many shaded, suppressed or fallen trees were not detected. On narrow roads with forest on both sides, some false detections were also recorded, but the number of such false detections is considered as negligible.

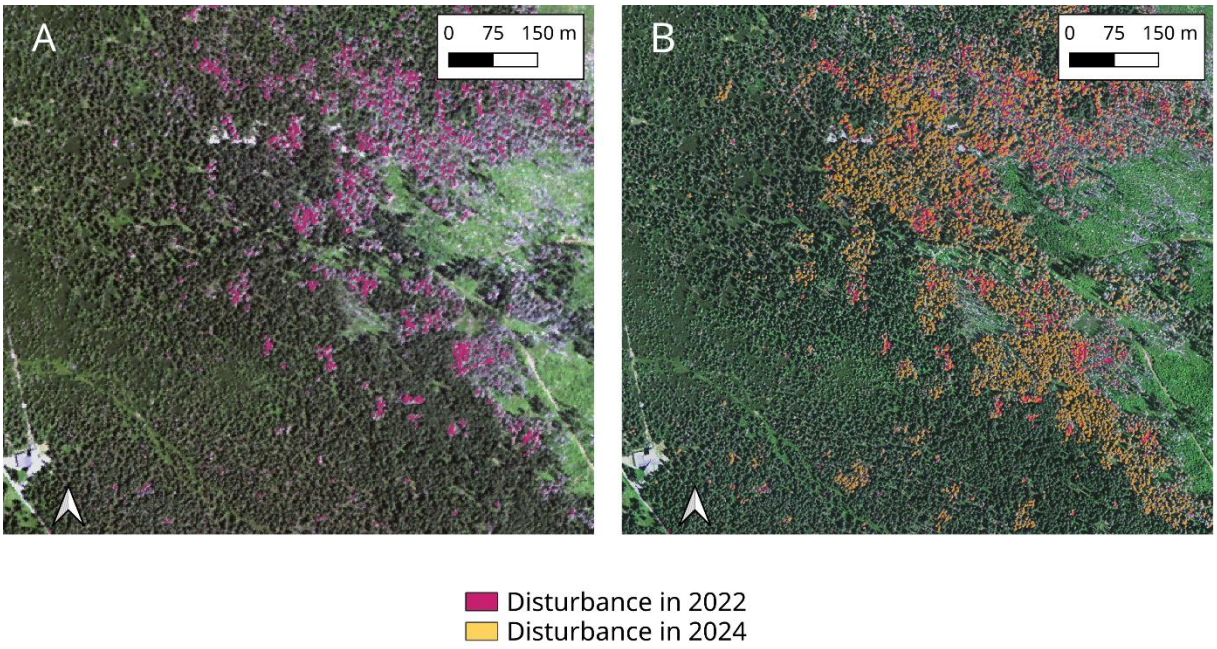

Fig. 2. *Detection of disturbances from airborne hyperspectral data at the sub-area A covered by airborne images in 2022 (A) and in 2024 (B).*

The satellite detection was based on a DI slope value threshold of 0.5. The choice of this threshold was supported by our previous research and other studies (Kupková et al. 2018; Mildrexler et al. 2009). We achieved a high agreement with the airborne detection as is shown in Fig. 3 A. The uncertainties and errors in the georeferencing of both satellite and aerial images caused spatial shifts between detected disturbance from the two data sources (Fig. 3 A). Rather than pixel by pixel comparison, it is more appropriate to build a buffer zone around each detection.

Detection using satellite imagery alone tends to result in more false detections in areas of recent clearcutting or areas with low tree density (Fig. 3 B). Filtering by the precise mask of forest height did not suppress the number of false detections, because the background spectral reflectance (of dry needles or bare soil) have significantly affected the spectral information in the whole pixel or even of the adjacent pixels. The size of the Sentinel-2 pixels did not allow detecting small incipient disturbances, especially if they were isolated and more distant from already existing disturbances (Fig. 3 B).

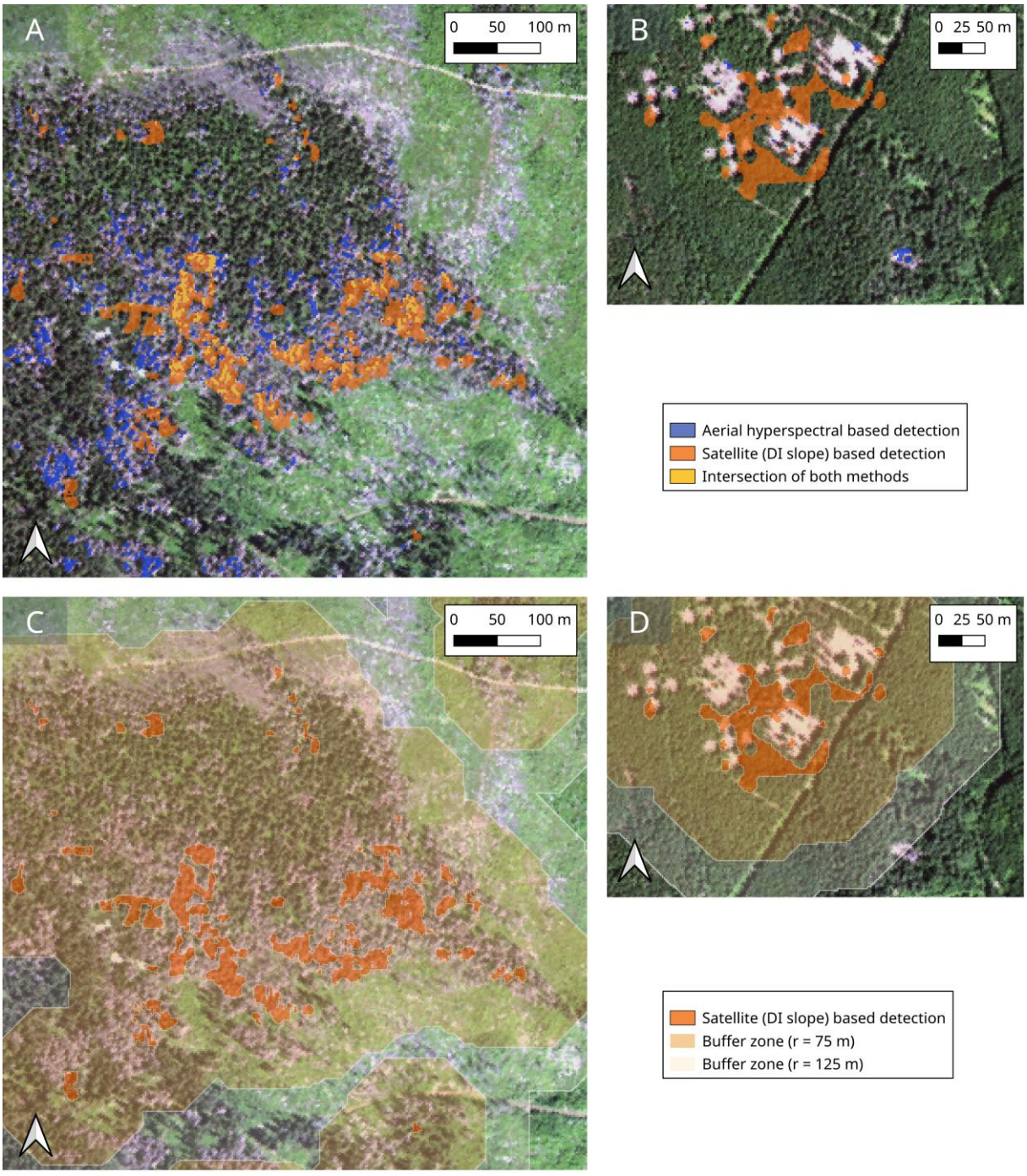

Fig. 3. *Detection of disturbances using satellite (orange colour) and airborne hyperspectral (blue colour) data in 2022. The buffer zones were constructed around the detected centres of disturbance at distances of 75, 125 m. The detection of disturbances of larger size is shown in section A. The false detection of disturbances with standing trees from satellite data and omitting disturbances of smaller size in the section B.*

3.2. Spatial progress of disturbances

Spatial progress was explored in disturbance epicentre (i.e. airborne detection) and four buffer zones around by observing the mean DI slope value (Fig. 4). The highest values of DI slope were located in the disturbance epicentre, these values decreased sharply with distance. This trend was apparent in all observed periods (i.e. 2017-2022, 2017-2023, and 2017-2024), the gradual increase in DI slope values in the centre of disturbance over the time indicated that the disturbance has not yet affected the whole area (Fig. 4A). The disturbance continued to spread into the surrounding area. This progress is relatively slow and space-limited because it mostly affects areas within 750 m (i.e. up to buffer zone r = 750 m) from the disturbance centres (Fig. 4B).

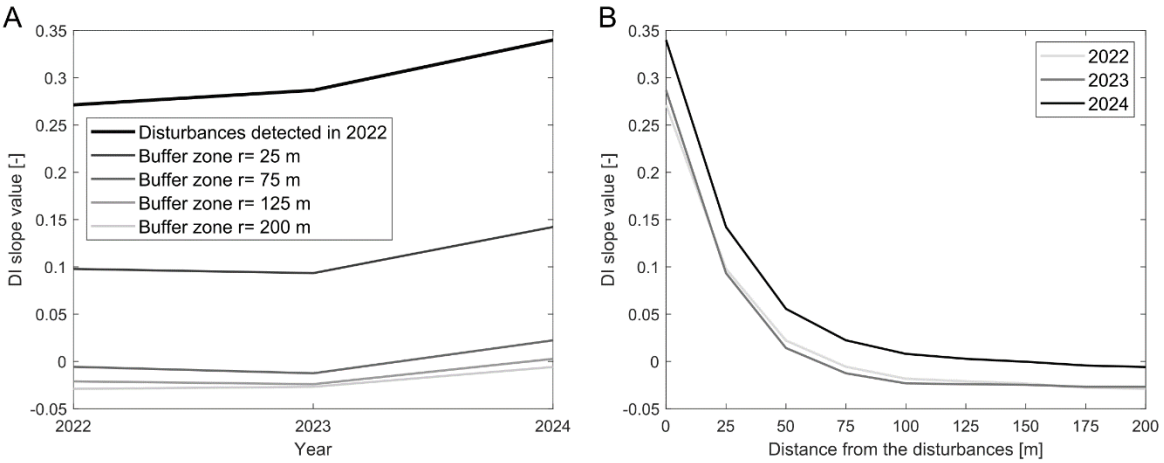

Fig. 4. *Development of satellite DI slope values in buffer zones around the disturbance pixels detected by airborne hyperspectral data in 2022. (a) Differences between buffer zones in time for selected zones, (b) decline of DI with the distance from detected disturbances.*

The comparison of initial spots under disturbances in 2022 and newly established spots in 2024 showed that 88.01 % of new spots were located within a distance of 75 m from initial spots (Fig. 5A). The percentage increases slowly with distance, where 92.67% of new disturbances were included within a distance of 100 m and 95.24% within a distance of 125 m. The time progress of a disturbance also affected the overall percentage, the areas in incipient phase of disturbance (sub-area B) showed lower percentages at all distances (i.e. 57.16 % within 75m, 66.92% within 100 m and 75.98% within 125 m) compared to areas with existing disturbances from previous years (sub-area A).

The median distance between the new and old disturbance spots for both areas was 25.88 m (Fig. 5B), the sub-area A with existing disturbance reaching 22.78 m and the sub-area B with disturbance in incipient phase reaching 88.27 m. As the majority of new disturbances were detected in sub-area A, which is also larger, the overall results reflected more the situation in sub-area A. Even if we considered the most extreme values, the maximum distance exceeded 250 m in only a few cases at both locations.

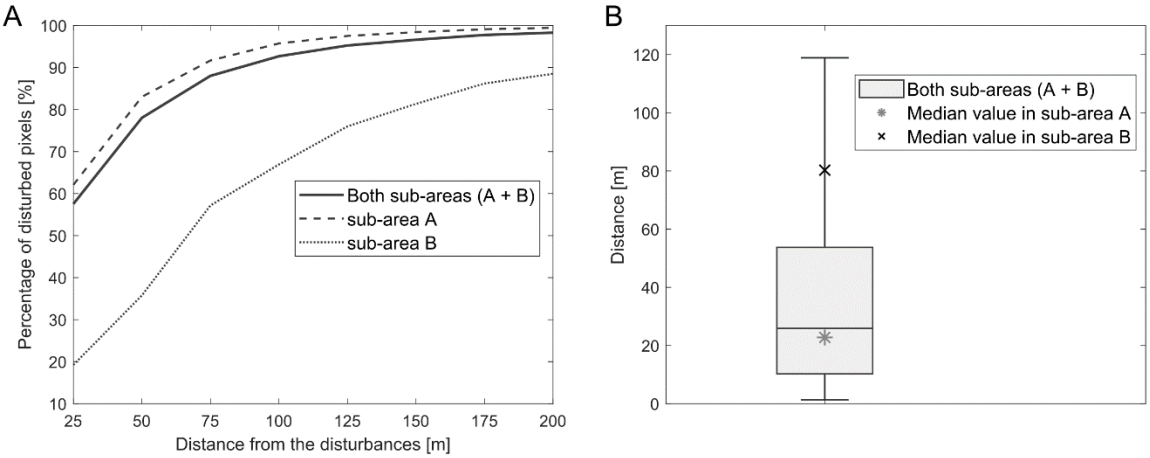

Fig. 5. *Spatial progress of disturbances detected from airborne hyperspectral data between years 2022 and 2024. (A) Cumulative sum of newly detected disturbances (based on 2024 data) depending on the distance from the epicentres detected in 2022. (B) Distribution of mean distance between epicentres detected in 2022 and newly detected disturbances in 2024. The mean distance was computed from the pixel detected as disturbance in 2024 to the 50 nearest pixels detected in 2022 (B).*

4. Discussion

4.1. Detection of disturbances

The detection of forest disturbance (dead standing trees) based on VNIR airborne data achieved overall accuracy of 87% in 2022 and 95% in 2024. Differences in the classification accuracy achieved between years can be explained by differences in spatial resolution, the classification using data with a spatial resolution of 2 m per pixel tended to result in more false detections due to mixed pixels.. Especially where the dead standing trees occurred on bare soil, unpaved roads, timber stacks and dead lying wood. Similar accuracies, and also confusion between dead standing trees and bare soil related classes was reported by Fassnacht et al. (2014) who used support vector machines to classify bark beetle induced tree mortality with airborne hyperspectral data in Bavarian Forest National Park. Alternatively, detection of dead standing

trees can be based on the combination of individual tree detection from airborne laser scanning data with optical spectral data (Jutras-Perreault et al., 2023). Using this approach might be challenging in topographically diverse areas with steep slopes, like our study area is, where geolocation errors between airborne laser scanning and optical data can occur. In addition, accuracy of individual tree detection can decrease on steep slopes (Khosravipour et al., 2015). The classification on merged VNIR and SWIR data did not result in higher accuracy in any case, likely because of the larger pixel size of the SWIR data.

The detection based on satellite data is proven to be an effective tool for mapping forest disturbances of a larger size, with the affected area larger than the spatial resolution of one pixel (Bárta et al., 2021, Fernandez-Carrillo et al., 2020). The success rate of detecting dead standing trees is usually around 90% (Fernandez-Carrillo et al., 2020; Fassnacht et al. 2014). These studies investigated detection possibilities in production forests, but their findings should be applicable to non-productive forests as well. Because the KRNAP spruce forests are characterized by lower tree density, smaller crown size and smaller height, it is assumed that the classification accuracy might be slightly lower here. Small incipient disturbances affecting a single group of trees were also mostly not captured by satellite data as is shown in Fig. 3B. Here, it is more profitable to use sensors with higher spatial resolution mounted on the airborne platform of UAV. In any case, the biggest disadvantage of using satellite data for disturbance detection is the high number of false detections out of forest areas. To minimize the number of false detections, the mask of tree height was used, which decreased the number of false detections on the meadow or on in places with rocky background. If the tree height mask was not available, it would be replaced by other sources for determining forest boundaries (e.g., forest management plan) to reduce false positives associated with non-forest objects.

Despite the above-mentioned disadvantages, the free availability of Sentinel-2 data, its large coverage in a single pass and the frequent revisiting time (every 5 days) makes satellite-based detection highly valuable for practical use. Then, the DI slope value-based detection method could be used for disturbance detection, from our experience the disturbance-related areas correspond to the threshold of 0.5. In another study, Kupková et al. (2018) reported mean DI values around 0.37 in heavily impacted areas during peak disturbance periods in the Ore Mts. (Czech Republic), suggesting that a threshold of 0.5 would encompass substantial canopy changes. Similarly, a study utilizing MODIS data over forests in North America established a 65% threshold for instantaneous disturbances monitored using MODIS Global Disturbance Index (Mildrexler et al., 2009), which, when normalized, corresponds to a DI value near 0.5.

The results of such detection should be verified through field survey observations, and areas with a higher risk of disturbance spreading should be intensively monitored by forest workers or by airborne or UAVs sensors.

4.2. Spatial progress

Buffer zones around each existing disturbance spot were defined to make monitoring of disturbance spread more efficient. This approach is based on the assumption that the distance from previous-year disturbances is considered as the main factor in determining the risk of subsequent tree mortality (Kautz et al., 2011; Potterf et al., 2019). Our results showed that progression into the immediate vicinity was also more probable and declined sharply with distance (Fig. 4). Potterf et al. (2019), who investigated bark beetle infestation progression in northern Slovakia, reported the same findings and stated that decline followed an inverse power-law function during peak and decline disturbance phases. In our study, the decline was found to slow significantly at a distance of approximately 75 meters on site under progression disturbance and 125 meters on site under incipient disturbance, forest stands within distance of 100m were identified as areas with higher risk of pests' damage (Kautz et al., 2011; Potterf et al., 2019). Kautz et al. (2011) reported that on average 65% of new bark beetle-killed trees were placed within a 100 m radius, and 95% trees within 500 m. Wichmann and Ravn (2001) extended this distance up to 500 m and reported that all old attacks are found within 500 m of a new attack. Wermelinger (2004) gives a range of 100 - 1500m in his review, but most studies after him tend towards the lower end of the range. Stadelmann et al. (2014) reported a distance of less than 500 m for new infestation spots, while Lausch et al. (2012) reported a mean distance of 116.45 m. The population density of bark beetles, whether endemic or epidemic, affects the strategy used to colonise trees, thereby affecting the range of areas at risk (Doležal et al., 2016; Hlásny et al., 2019; Wermelinger, 2004). During the endemic phase, the beetles tend to find susceptible trees over a wider range; they prefer trees with poor defence mechanisms. Meanwhile, during the epidemic phase, they can attack even healthy trees, with a high chance of successive attacks. This finding supports studies focusing on the flying capability of bark beetles, which reported that the number of marked beetles captured decreased exponentially with increasing distance from the release point (Doležal et al., 2016). The success of bark beetle attack depends on many factors, such as tree vigour, spatial distribution of susceptible trees or population density (Hlásny et al., 2019). However, it is still not possible to predict future spots of infestation (Stereńczak et al., 2014).

There is no doubt that the distance gradient depends on the disturbance phase. This was demonstrated in sub-areas A and B: sub-area A, being in a peak phase, showed a shorter average distance of 22.78 meters between old and new disturbance spots, while sub-area B, which was in an emerging phase, exhibited a greater average distance of 88.27 meters between the same categories. This is consistent with the findings of other studies, who investigated the disturbance progression in natural protected areas (Kautz et al., 2011; Potterf et al., 2019). The disturbance progression is undoubtedly influenced by other factors like slope orientation, forest age structure, species composition, wind direction or amount of precipitation affecting tree vigour. Due to the lack of additional data the small extent of studies areas we have not evaluated the influence of those factors.

5. Conclusion

In this study we analysed spatial patterns and progress of forest disturbances in a specific forest ecosystem - mountain Norway spruce forests in the KRNAP national park in the Czech Republic, where standard forest management practices are either very limited or even absent compared to typical Central European production spruce forests. The forest disturbances, declining and dead standing trees, most likely caused by bark beetle infestation, were analysed from airborne hyperspectral data and Sentinel-2 data. We evaluated the spatial progress of disturbances between 2022 and 2024 by analysing buffer zones constructed around the epicentres of disturbances detected in 2022. The probability of the occurrence of new disturbances and progress of the existing ones decreases with the distance from the detected disturbances. Both remote sensing data sources confirmed that the buffer zone of up to 125 m is the most critical zone to inspect for new or progressing disturbances. In areas where disturbances begin, it is necessary to expand this zone up to 200 m to inspect and identify newly declining trees in a wider perimeter. The establishing of perimeters could help forest workers to plan field surveys in areas with difficult terrain. As a starting point for the creation of these buffer zones, a disturbance detection based on satellites, airplanes or UAVs data could be used. Despite the fact that the distance of critical zones around existing disturbances corresponds to findings of other studies, its range depends on forest distribution in a specific landscape.

Acknowledgments

This work was supported by the Technology Agency of the Czech Republic, Assessment of the impact of land cover changes on local hydrology and climate in the Krkonoše Mts. National Park using remote sensing (SS05010124) and by the European Commission, CINEA Horizon

Europe project no. 101081307 “Towards Sustainable Land-Use in the Context of Climate Change and Biodiversity in Europe (Europe-LAND)”. We also want to thank our colleagues of the Krkonoše National Park Administration, specifically Václav Jansa and Roman Rejzek.

References

Bárta, V., Lukeš, P., Homolová, L., 2021. Early detection of bark beetle infestation in Norway spruce forests of Central Europe using Sentinel-2. International Journal of Applied Earth Observation and Geoinformation 100, 102335. https://doi.org/10.1016/j.jag.2021.102335

Bijou, S., Kupková, L., Potůčková, M., Červená, L., Lysák, J., 2023. Evaluation of the Bark Beetle Green Attack Detectability in Spruce Forest from Multitemporal Multispectral UAV Imagery. ISPRS Annals of the Photogrammetry, Remote Sensing and Spatial Information Sciences X-1-W1-2023, 1033–1040. https://doi.org/10.5194/isprs-annals-X-1-W1-2023-1033-2023

Brázdil, R., Zahradník, P., Szabó, P., Chromá, K., Dobrovolný, P., Dolák, L., Trnka, M., Řehoř, J., Suchánková, S., 2022. Meteorological and climatological triggers of notable past and present bark beetle outbreaks in the Czech Republic. Climate of the Past 18, 2155–2180. https://doi.org/10.5194/cp-18-2155-2022

Byers, J.A., 2000. Wind-aided dispersal of simulated bark beetles flying through forests. Ecol. Model. 125, 231–243. https://doi.org/10.1016/S0304-3800(99)00187-8

ClimRisk, 2025. Web-based portal to view climatic data for the Czech Republic. URL https://www.climrisk.eu/mapa-cr/ (accessed 18. 7. 2025)

Copernicus Service, 2021. Copernicus Sentinel-2 Collection 1 MSI Level-2A. [WWW Document]. Sentinel Online. URL https://sentinels.copernicus.eu/sentinel-data-access/sentinel-products/sentinel-2-data-products/collection-1-level-2a (accessed 5.5.25).

Doležal, P., Okrouhlík, J., Davídková, M., 2016. Fine fluorescent powder marking study of dispersal in the spruce bark beetle, Ips typographus (Coleoptera: Scolytidae). European Journal of Entomology 113, 1–8. https://doi.org/10.14411/eje.2016.001

Drechsel, J., Forkel, M., 2025. Remote sensing forest health assessment – a comprehensive literature review on a European level. Central European Forestry Journal 71, 14–39. https://doi.org/10.2478/forj-2024-0022

Fassnacht, F.E., Latifi, H., Ghosh, A., Joshi, P.K., Koch, B., 2014. Assessing the potential of hyperspectral imagery to map bark beetle-induced tree mortality. Remote Sensing of Environment 140, 533–548. https://doi.org/10.1016/j.rse.2013.09.014

Fernandez-Carrillo, A., Patočka, Z., Dobrovolný, L., Franco-Nieto, A., Revilla-Romero, B., 2020. Monitoring Bark Beetle Forest Damage in Central Europe. A Remote Sensing Approach Validated with Field Data. Remote Sensing 12, 3634. https://doi.org/10.3390/rs12213634Gorelick, N., Hancher, M., Dixon, M., Ilyushchenko, S., Thau, D., Moore, R., 2017. Google Earth Engine: Planetary-scale geospatial analysis for everyone. Remote Sensing of Environment, Big Remotely Sensed Data: tools, applications and experiences 202, 18–27. https://doi.org/10.1016/j.rse.2017.06.031

Hallas, T., Steyrer, G., Laaha, G., Hoch, G., 2024. Two unprecedented outbreaks of the European spruce bark beetle, Ips typographus L. (Col., Scolytinae) in Austria since 2015: Different causes and different impacts on forests. Central European Forestry Journal 70, 263–274. https://doi.org/10.2478/forj-2024-0014

Hanuš, J., Slezák, L., Fabiánek, T., Fajmon, L., Hanousek, T., Janoutová, R., Kopkáně, D., Novotný, J., Pavelka, K., Pikl, M., Zemek, F., Homolová, L., 2023. Flying Laboratory of Imaging Systems:

Fusion of Airborne Hyperspectral and Laser Scanning for Ecosystem Research. Remote Sensing 15, 3130. https://doi.org/10.3390/rs15123130

Healey, S.P., Cohen, W.B., Zhiqiang, Y., Krankina, O.N., 2005. Comparison of Tasseled Cap-based Landsat data structures for use in forest disturbance detection. Remote Sensing of Environment 97, 301–310. https://doi.org/10.1016/j.rse.2005.05.009

Hlásny, T., Krokene, P., Liebhold, A., Montagné-Huck, C., Müller, J., Qin, H., Raffa, K., Schelhaas, M-J., Seidl, R., Svoboda, M., Viiri, H. 2019. Living with bark beetles: impacts, outlook and management options. From Science to Policy 8. Report. European Forest Institute. https://doi.org/10.36333/fs08

Hlásny, Tomáš, König, L., Krokene, P., Lindner, M., Montagné-Huck, C., Müller, J., Qin, H., Raffa, K.F., Schelhaas, M.-J., Svoboda, M., Viiri, H., Seidl, R., 2021a. Bark Beetle Outbreaks in Europe: State of Knowledge and Ways Forward for Management. Curr Forestry Rep 7, 138–165. https://doi.org/10.1007/s40725-021-00142-x

Hlásny, T., Zimová, S., Merganičová, K., Štěpánek, P., Modlinger, R., Turčáni, M., 2021b. Devastating outbreak of bark beetles in the Czech Republic: Drivers, impacts, and management implications. Forest Ecology and Management 490, 119075. https://doi.org/10.1016/j.foreco.2021.119075

Jutras-Perreault, M.-C., Næsset ,Erik, Gobakken ,Terje, and Ørka, H.O., 2023. Detecting the presence of standing dead trees using airborne laser scanning and optical data. Scandinavian Journal of Forest Research 38, 208–220. https://doi.org/10.1080/02827581.2023.2211807

Kautz, M., Dworschak, K., Gruppe, A., Schopf, R., 2011. Quantifying spatio-temporal dispersion of bark beetle infestations in epidemic and non-epidemic conditions. Forest Ecology and Management 262, 598–608. https://doi.org/10.1016/j.foreco.2011.04.023

Khosravipour, A., Skidmore, A.K., Wang, T., Isenburg, M., Khoshelham, K., 2015. Effect of slope on treetop detection using a LiDAR Canopy Height Model. ISPRS Journal of Photogrammetry and Remote Sensing 104, 44–52. https://doi.org/10.1016/j.isprsjprs.2015.02.013

Kirby, K.J., Watkins, C. (Eds.), 2015. Europe's changing woods and forests: from wildwood to managed landscapes. CABI.

Kupková, L., Potůčková, M., Lhotáková, Z., Albrechtová, J., 2018. Forest cover and disturbance changes, and their driving forces: A case study in the Ore Mountains, Czechia, heavily affected by anthropogenic acidic pollution in the second half of the 20th century. Environ. Res. Lett. 13, 095008. https://doi.org/10.1088/1748-9326/aadd2c

Kusbach A., Krejza, J., Homolová, L., Fischer, M., Janoutová, R., Horáček, P., 2025. Productivity of coniferous forests evaluated by remote sensing and field-based models. Environ. Res. Lett. 20, 024016. https://doi.org/10.1088/1748-9326/ada2af

Lausch, A., Heurich, M., Fahse, L., 2013. Spatio-temporal infestation patterns of Ips typographus (L.) in the Bavarian Forest National Park, Germany. Ecological Indicators, Linking landscape structure and biodiversity 31, 73–81. https://doi.org/10.1016/j.ecolind.2012.07.026

Mildrexler, D.J., Zhao, M., Running, S.W., 2009. Testing a MODIS Global Disturbance Index across North America. Remote Sensing of Environment 113, 2103–2117. https://doi.org/10.1016/j.rse.2009.05.016

Montagné-Huck, C., Brunette, M., 2018. Economic analysis of natural forest disturbances: A century of research. JFE 32, 42–71. https://doi.org/10.1016/j.jfe.2018.03.002

Müller, J., Bußler, H., Goßner, M., Rettelbach, T., Duelli, P., 2008. The European spruce bark beetle Ips typographus in a national park: from pest to keystone species. Biodivers Conserv 17, 2979–3001. https://doi.org/10.1007/s10531-008-9409-1

MZE, 2024. Zpráva o stavu lesa a lesního hospodářství České Republiky v roce 2023 (Report on the state of forests and forestry in the Czech Republic in 2023). Ministry of Agriculture of the Czech Republic. ISBN 978-80-7434-790-0. Report in Czech. Available online:

https://mze.gov.cz/public/portal/mze/publikace/zprava-o-stavu-lesa-a-lesniho-hospodarstvi-cr/zprava-o-stavu-lesa-a-lesniho-hospodarstvi-2023 (accessed 2.7.2025)

Nikolov, C., Konôpka, B., Kajba, M., Galko, J., Kunca, A., Janský, L., 2014. Post-disaster Forest Management and Bark Beetle Outbreak in Tatra National Park, Slovakia. mred 34, 326–335. https://doi.org/10.1659/MRD-JOURNAL-D-13-00017.1

Økland, B., Nikolov, C., Krokene, P., Vakula, J., 2016. Transition from windfall- to patch-driven outbreak dynamics of the spruce bark beetle Ips typographus. Forest Ecology and Management 363, 63–73. https://doi.org/10.1016/j.foreco.2015.12.007

Patacca, M., Lindner, M., Lucas-Borja, M.E., Cordonnier, T., Fidej, G., Gardiner, B., Hauf, Y., Jasinevičius, G., Labonne, S., Linkevičius, E., Mahnken, M., Milanovic, S., Nabuurs, G.-J., Nagel, T.A., Nikinmaa, L., Panyatov, M., Bercak, R., Seidl, R., Ostrogović Sever, M.Z., Socha, J., Thom, D., Vuletic, D., Zudin, S., Schelhaas, M.-J., 2023. Significant increase in natural disturbance impacts on European forests since 1950. Global Change Biology 29, 1359–1376. https://doi.org/10.1111/gcb.16531

Potterf, M., Nikolov, C., Kočická, E., Ferenčík, J., Mezei, P., Jakuš, R., 2019. Landscape-level spread of beetle infestations from windthrown- and beetle-killed trees in the non-intervention zone of the Tatra National Park, Slovakia (Central Europe). Forest Ecology and Management 432, 489–500. https://doi.org/10.1016/j.foreco.2018.09.050

Seidl, R., Schelhaas, M.-J., Lexer, M.J., 2011. Unraveling the drivers of intensifying forest disturbance regimes in Europe. Global Change Biology 17, 2842–2852. https://doi.org/10.1111/j.1365-2486.2011.02452.x

Seidl, R., Thom, D., Kautz, M., Martin-Benito, D., Peltoniemi, M., Vacchiano, G., Wild, J., Ascoli, D., Petr, M., Honkaniemi, J., Lexer, M.J., Trotsiuk, V., Mairota, P., Svoboda, M., Fabrika, M., Nagel, T.A., Reyer, C.P.O., 2017. Forest disturbances under climate change. Nature Clim Change 7, 395–402. https://doi.org/10.1038/nclimate3303

Senf, C., Seidl, R., 2021. Mapping the forest disturbance regimes of Europe. Nat Sustain 4, 63–70. https://doi.org/10.1038/s41893-020-00609-y

Senf, C., Seidl, R., Hostert, P., 2017. Remote sensing of forest insect disturbances: Current state and future directions. International Journal of Applied Earth Observation and Geoinformation 60, 49–60. https://doi.org/10.1016/j.jag.2017.04.004

Sentinel Hub, 2025. Sentinel Hub Cloud Detector for Sentinel-2 images. Python package s2cloudless [WWW Document]. URL https://github.com/sentinel-hub/sentinel2-cloud-detector (accessed 5.5.25).

Stadelmann, G., Bugmann, H., Wermelinger, B., Bigler, C., 2014. Spatial interactions between storm damage and subsequent infestations by the European spruce bark beetle. Forest Ecology and Management 318, 167–174. https://doi.org/10.1016/j.foreco.2014.01.022

Stereńczak, K., Mielcarek, M., Modzelewska, A., Kraszewski, B., Fassnacht, F.E., Hilszczański, J., 2019. Intra-annual Ips typographus outbreak monitoring using a multi-temporal GIS analysis based on hyperspectral and ALS data in the Białowieża Forests. Forest Ecology and Management 442, 105–116. https://doi.org/10.1016/j.foreco.2019.03.064

Thom, D., Seidl, R., Steyrer, G., Krehan, H., Formayer, H., 2013. Slow and fast drivers of the natural disturbance regime in Central European forest ecosystems. Forest Ecology and Management 307, 293–302. https://doi.org/10.1016/j.foreco.2013.07.017

Vrba, P., Beneš, J., Čížek, L., Filippov, P., Faltýnek Fric, Z., Hauck, D., Konvička, M., Spitzer, L., 2024. Bark beetle outbreak and biodiversity in commercial spruce plantations: Responses of four model groups. Forest Ecology and Management 555, 121700. https://doi.org/10.1016/j.foreco.2024.121700

Wermelinger, B., 2004. Ecology and management of the spruce bark beetle Ips typographus—a review of recent research. Forest Ecology and Management 202, 67–82. https://doi.org/10.1016/j.foreco.2004.07.018

Wichmann, L., Ravn, H.P., 2001. The spread of Ips typographus (L.) (Coleoptera, Scolytidae) attacks following heavy windthrow in Denmark, analysed using GIS. Forest Ecology and Management 148, 31–39. https://doi.org/10.1016/S0378-1127(00)00477-1

Zahradník, P., Zahradníková, M., 2019. Salvage felling in the Czech Republic‘s forests during the last twenty years. Central European Forestry Journal 65, 12–20. https://doi.org/10.2478/forj-2019-0008